MICROMECHANICAL MODELLING AND SIMULATION OF TRIANGLE-SECTION CARBON FIBER REINFORCED POLYMER COMPOSITES

Lei Yang, Zhanjun Wu and Xin Liu

State Key Laboratory of Structural Analysis for Industrial Equipment, School of Aeronautics and Astronautics, Dalian University of Technology, Dalian 116024, PR China
E-mail: yangl@dlut.edu.cn, Web Page: http://en.dlut.edu.cn/

Keywords: Triangle-section carbon fiber, Representative volume element (RVE), Finite element method (FEM), Micromechanics, Damage mechanism

Abstract
The physical and mechanical properties of carbon fiber reinforced plastics (CFRPs) are dependent largely on the fiber content, the fiber orientation, and the cross-section shape of fibers. Generally, the cross-section shape of the reinforcing fibers in composites is round-shape. However, from the viewpoint of structural mechanics, it is recognized that non-round-shape fiber will do well than round-shape fiber in mechanical properties of CFRPs, because the non-round-shape carbon fibers have higher specific surface area than the conventional round-shape carbon fibers. Besides, for composites reinforced by triangle-shape carbon fibers, the fibers in the composites can reflect incidence microwave many times as its microstructure can work like anechoic chamber, contributing to higher absorbing ratio of electro-magnetic wave. In order to reveal the effect of triangle-section fiber on the mechanical properties of CFRPs, micromechanical model of the composites based on representative volume element (RVE) was developed in this paper. The mechanical properties and damage behavior of unidirectional triangle-section fiber-reinforced polymer composites under transverse tension and compression were simulated. The simulation results clearly reveal the microscopic damage mechanisms of the triangle-section fiber-reinforced polymer composites.

1. Introduction

Over the past few decades carbon fiber reinforced plastics (CFRPs) have been increasingly used in aerospace [1] and other industries [2] for their high specific stiffness, high specific strength, and outstanding designability. The physical and mechanical properties of CFRP are dependent largely on the fiber content, the fiber orientation, and the cross-section shape of fibers [3]. Generally, the cross-section shape of the reinforcing fibers in composites is round-shape. However, from the viewpoint of structural mechanics, it is recognized that non-round-shape fiber will do well than round-shape fiber in mechanical properties of CFRPs, because the non-round-shape carbon fibers have higher specific surface area than the conventional round-shape carbon fibers (RCFs). The larger area in the surface contacting with the matrix can increase the interfacial bonding force, consequently improve the mechanical properties of the composites [4]. Besides, in some fields, non-round-shape carbon fiber reinforced composites may be better choice for their special properties. For example, for composites reinforced by triangle-shape carbon fibers (TCFs), the TCFs in the composites can reflect incidence microwave many times as its microstructure can work like anechoic chamber [5], contributing to higher absorbing ratio of electro-magnetic wave. Therefore, with good mechanical properties and wave-absorbing properties, the triangle-shape carbon fiber reinforced plastics (TCFRPs) are very promising structural and functional materials.

Excerpt from ISBN 978-3-00-053387-7

However, up to date, there are only a limited number of studies on the non-round-shape carbon fibers and their composites. Park et al. [6-8] studied the mechanical properties of various shapes of carbon fibers reinforced cement composites. They found that C-shape carbon fiber reinforced cement composites showed higher tensile and flexural strength than round-shape and any other shape carbon fibers reinforced composites. Xu et al. [9-10] conducted a comprehensive experimental study to identify the differences of the kidney section carbon fibers and circular section carbon fibers in the surface characteristics of fibers and mechanical properties of composites. It was revealed that the kidney fibers with larger specific surface area have a better adsorption characteristic and higher impregnating performance compared with the circular fibers. Pakravan et al. [11] studied the influence of acrylic fibers shape on the flexural behavior of cement composite. It was found that by increasing the fibers' shape factor, both flexural strength and toughness of the composite increased. In the previous work, the authors [4] manufactured the triangle-shape carbon fiber reinforced plastics, as shown in Fig.1, and their flexural properties were experimentally investigated. It was found that the TCFRPs showed higher flexural strength and flexural modulus than round-shape carbon fiber reinforced plastics, and the tensile strength and tensile modulus did not reduce.

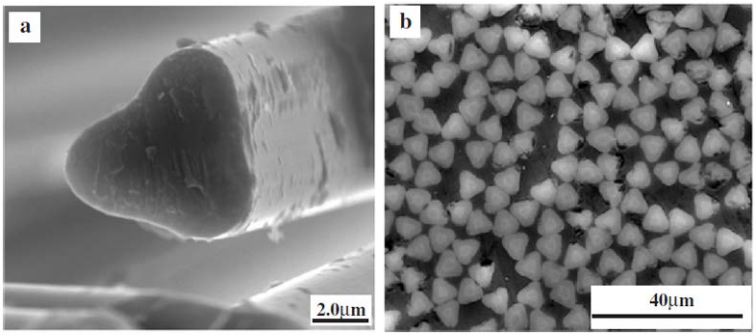

Figure 1. SEM micrographs of triangle-section carbon fiber and the composites

In order to thoroughly understand the effect of fiber shape on the mechanical properties of CFRPs, a micromechanics approach based on numerical method is a good choice to reveal the intrinsic mechanisms of this effect. Many researchers have presented various micromechanics approaches [12-15]. The authors previously developed a micromechanical model for fiber reinforced plastics [16], which can precisely simulate the mechanical and damage behavior of unidirectional fiber-reinforced polymer composites. In this study, this model is used to simulate the micromechanical and damage behavior of unidirectional TCFRPs subjected to transverse tension and compression loads. The stress-strain curves of the composites were generated and the tensile and compressive strength were obtained.

2. Modeling strategies

2.1. FEM model

To perform micromechanical analysis of composites, a representative volume element (RVE) of the microstructure large enough to possess the same properties with the macroscopic material should be generated. From Fig.1 it can be seen that the fibers are randomly embedded in the matrix, which should be taken into account in the RVE of composites. From the figure it can also be seen that the section of triangle fiber is not an exact triangle, but with fillet at each vertex. These fillets were naturally formed during the manufacture process of the fibers, thus should be retained in the RVE.

The random distribution of fibers in the RVE is generated by the random sequential expansion (RSE) algorithm [17] developed by the authors. Shown in Fig.2a are one of the generated RVE of TCFRPs,

Excerpt from ISBN 978-3-00-053387-7

each RVE containing 30 fibers [18], with fiber volume fraction of 50%. The side length of the triangle-shape fibers is 10 μm, and the fillet radius is 1.6 μm. Five separate RVEs with different fiber distributions are generated for the TCFRPs (TCF-1~TCF-5) to take into account the effect of microscopic configuration.

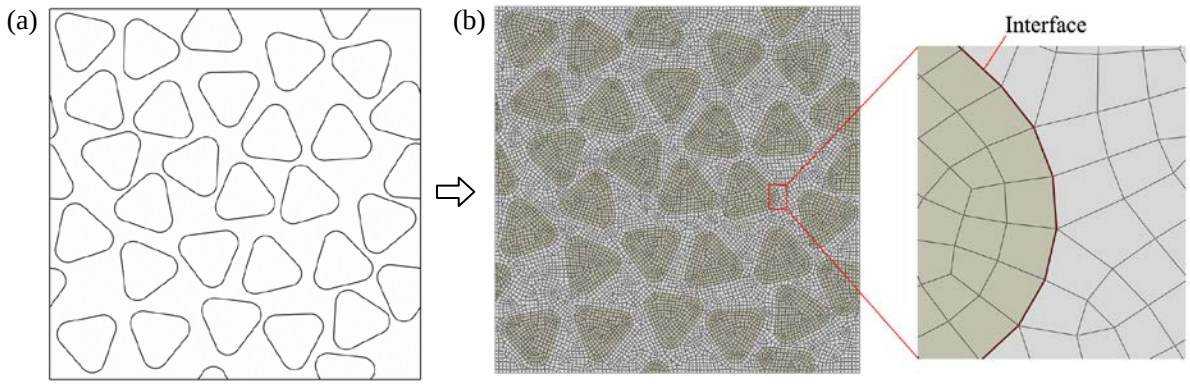

Figure 2. RVE TCF-1 and its mesh discretization

The modeling and simulation platform of the study is the FEM package ABAQUS. The fibers and matrix are meshed with 4-node bilinear plane strain quadrilateral, reduced integration elements. As the interface between fibers and matrix can have significant influence on the properties of the composites, a layer of 4-node two-dimensional cohesive elements with very small thickness (0.01μm) are introduced between each fiber and the surrounding matrix to simulate the interfacial debonding. Taking the RVE of TCF-1 as an example, shown in Fig.2b is the mesh discretization of TCF-1. Periodic boundary conditions are applied to the RVEs to ensure a macroscopically uniform stress/displacement field. Transverse tension or compression load is applied to the RVEs by giving a compulsive displacement along the horizontal direction.

2.2. Material models

The triangle-shape carbon fibers and the round-shape carbon fibers were supplied by Shanxi Institute of Coal Chemistry, China. The epoxy resin TDE-85 was supplied by Tianjin Resin Plant, China. Their transverse mechanical properties are listed in Table 1.

Table 1. Transverse mechanical properties of the carbon fiber and epoxy resin

Properties	Carbon fiber	Epoxy resin
Young's modulus (GPa)	23.34	3.45
Poisson's ratio	0.25	0.35
Tensile strength (MPa)	—	85.7
Compressive strength (MPa)	—	232.5

As fiber fracture is unlikely to happen under transverse loading, no damage behavior is considered for the carbon fibers, which are modelled as linear elastic and isotropic solids. The material and damage models for the matrix and interface have been discussed in detail in [16], and they are briefly described as follows.

Excerpt from ISBN 978-3-00-053387-7

The extended linear Drucker-Prager criterion is employed to predict the yielding of the matrix, including the effect of hydrostatic stress on yielding behaviour:

$$F = t - p\tan\beta - d = 0, \quad t = \frac{1}{2}q\left[1 + \frac{1}{k} - \left(1 - \frac{1}{k}\right)\left(\frac{r}{q}\right)^3\right] \tag{1}$$

where p is the hydrostatic stress, q is the Mises equivalent stress, r is the third invariant of deviatoric stress, β is the slope of the linear yield surface in the p–t stress plane, d is the cohesion of the material, and k is the ratio of the yield stress in triaxial tension to the yield stress in triaxial compression and, thus, introduces different yield behaviours between tension and compression.

The ductile criterion is used to predict the onset of damage for the matrix, which assumes the equivalent plastic strain at the onset of damage as a function of stress triaxiality η ($\eta = -p/q$), thus predicting the damage onset discriminating between different triaxial stress states. Here, the equivalent plastic strain at damage initiation for uniaxial tension $\bar{\varepsilon}_{0+}^{pl}$ ($\eta = 1/3$) and uniaxial compression $\bar{\varepsilon}_{0-}^{pl}$ ($\eta = -1/3$) are used to achieve different behaviors between tension and compression. After the onset of failure, the damage evolution is controlled by a progressive failure procedure based on energy criterion, with the fracture energy of the matrix defined as G_m. The damage manifests itself in two forms: softening of the yield stress and degradation of the elasticity, both of which are related to the damage variable that increases with the evolution of damage. The stress-strain response of the matrix is illustrated in Fig.3.

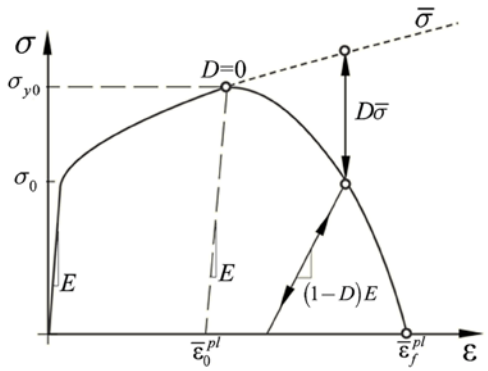

Figure 3. Stress-strain response of the matrix

The constitutive response of the cohesive element is defined in terms of a bi-linear traction-separation law which relates the separation displacement between the top and bottom faces of the element to the traction vector acting upon it. The initial response is linear in absence of damage with an elastic stiffness of K:

$$t_{n/s} = K_{n/s}\delta_{n/s} \tag{2}$$

The initiation of damage is predicted by the maximum stress criterion:

$$\max\left\{\frac{\langle t_n \rangle}{t_n^0}, \frac{t_s}{t_s^0}\right\} = 1 \tag{3}$$

where 〈 〉 is the Macaulay brackets, which return the argument if positive and zero otherwise, to impede the development of damage when the interface is under compression, and t_n^0 and t_s^0 are the normal and tangential interfacial strengths.

After damage onset, the traction stress is reduced depending on the interface damage parameter,

Excerpt from ISBN 978-3-00-053387-7

following a linear traction–separation law. The energy necessary to completely break the interface is equal to the interface fracture energy G_n (for Mode I damage) or G_s (for Mode II damage).

The involved material parameters used in the simulation for the matrix and interface are listed in Table 2. As the interface strength is very difficult to obtain by experiment, it is assumed that the normal and tangential interface strengths are identical and equal to the tensile strength of the matrix.

Table 2. Material parameters of the matrix and interface

Matrix	d (MPa)	β	k	$\bar{\varepsilon}_{0+}^{pl}$	$\bar{\varepsilon}_{0-}^{pl}$	G_m (J/m^2)
	104.8	37.7°	0.8	0.025	0.25	5
Interface	$K_n = K_s$ (GPa/m)		$t_n^0 = t_s^0$ (MPa)		$G_n = G_s$ (J/m^2)	
	10^8		85.7		100	

3. Results and discussion

3.1. Stress field

Shown in Fig.4 are the maximum principal stress contour plots of TCF-1 and TCF-2 respectively, at the loading level of 0.1% equivalent strain (the load is applied along the horizontal direction). As the loading level is very low, all the constituent materials are still in their elastic states, i.e., without plastic deformation and damage initiation. As can be seen, due to the significant distinction of elastic properties between fibers and matrix, stress concentration happens at the junction regions between fibers and matrix. Owing to the diversity of position relation between different triangle fibers, the microscopic stress field is complicated. But generally the maximum stress occurs at the locations where two fibers are closely adjacent. The maximum principal stress in TCF-2 (18.5 MPa) is higher than that in TCF-1 (17.6 MPa). However, the maximum stress is greatly influenced by the microscopic configuration of the RVE, especially the distance between fibers. And it is the overall stress field, instead of the maximum stress, that reflects the stiffness characteristic of the composites.

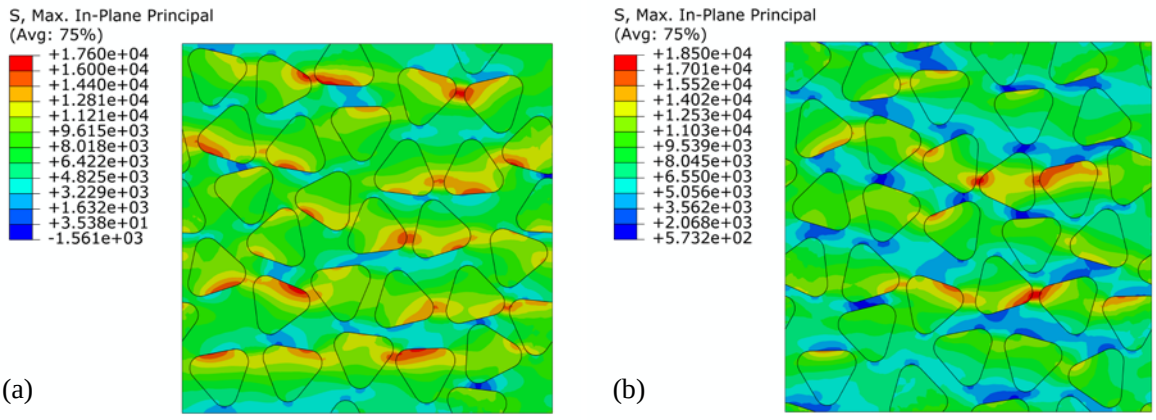

Figure 4. The stress contour plots of (a) TCF-1 and (b) TCF-2 at 0.1% equivalent strain (Unit: KPa)

3.2. Damage initiation and evolution

The simulation results can help to reveal the microscopic damage mechanisms of the composites, and explain how the fiber shape affects the damage behavior of the composites. Taking TCF-1for example,

Excerpt from ISBN 978-3-00-053387-7

shown in Fig.5a are the damage initiation and evolution process of the RVE under transverse tension. As can be seen, interfacial debonding first occurs at the vertex of the triangle fibers where the inter-fiber distance is small, as can be seen more clearly by the partial enlarged drawing. Then, matrix plastic damage begins to appear at the vicinity of the interfacial debonding, and more interfacial debonding occurs at other locations. Finally, the matrix cracks propagate along the edge of fibers, and interfacial debonding at different locations is linked by matrix cracks, forming a fold line matrix crack through the RVE and causing the ultimate fracture of the RVE.

For transverse compression, the damage initiation and evolution process of TCF-1 is illustrated in Fig.5b. As can be seen, the damage behavior is different from that of transverse tension: matrix plastic damage first happens at the location where two fibers are closely adjacent in the direction perpendicular to the load. Then, more matrix cracks occur at different locations, most adjoining the fibers. And finally the matrix cracks at different locations are linked to form a main crack, having a certain angle with the loading direction, which is called the plastic shear band. Thus it is concluded that the damage behavior of the composites under transverse compression is dominated by the matrix.

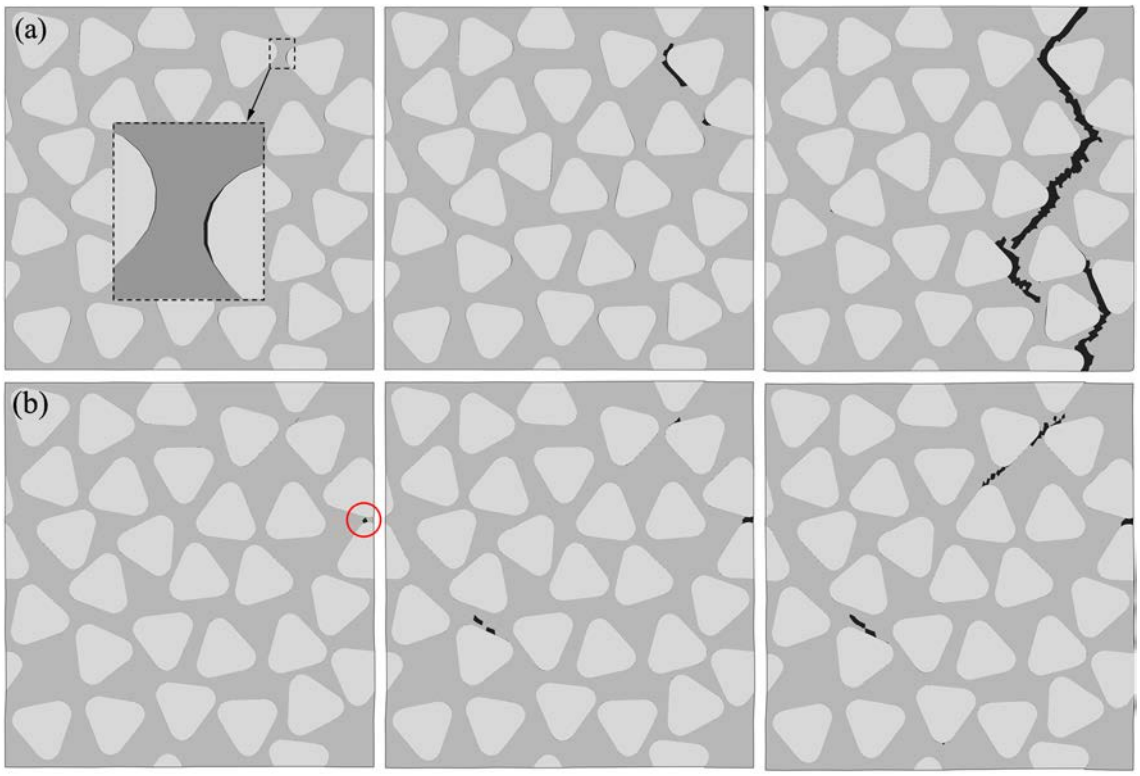

Figure 5. Damage initiation and evolution process of TCF-1 under:
(a) transverse tension; (b) transverse compression

3.3. Stress-strain curve

The stress-strain curves of all the five RVEs for TCFRPs under transverse tension are shown in Fig.6a. As can be seen, the initial stress-strain relation is almost linear, following with a short plastic stage, and then failure happens as a sudden drop in the stress-strain curves. For different RVEs, the elastic regimes of the curves are almost superposed, and divergence does not occur until the onset of damage. Shown in Fig.6b are the stress-strain curves of all the five RVEs for TCFRPs under transverse compression. Compared with transverse tension, there is more dispersion in the stress-strain curves between different RVEs.

Excerpt from ISBN 978-3-00-053387-7

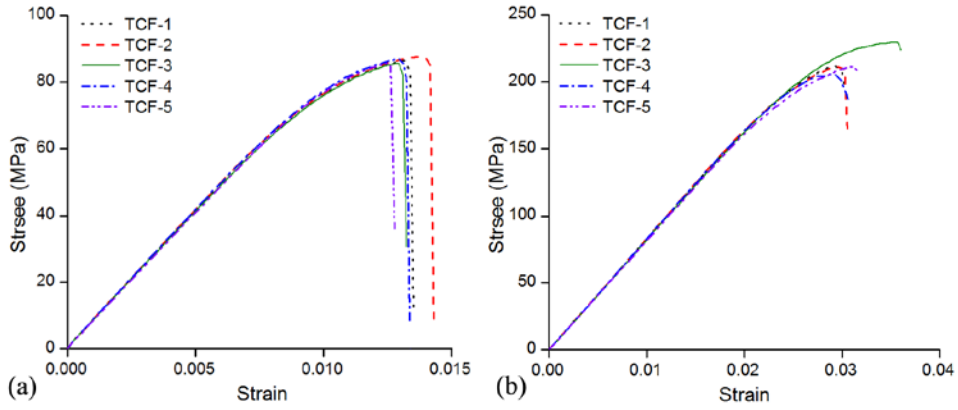

Figure 6. Stress-strain curves of TCFRPs under: (a) transverse tension; (b) transverse compression

4. Conclusions

The transverse mechanical properties and damage behavior of triangle-shape carbon fiber reinforced plastics were simulated by finite element analysis on the representative volume elements of CFRPs. The simulation results clearly reveal the microscopic failure mechanisms of the composites. Under transverse tension, with the increase of load, interfacial debonding first occurs at the vertex of the triangle fibers where the inter-fiber distance is small, and then matrix plastic damage happens at the vicinity of the interfacial debonding; finally, interfacial debondings at different locations are linked by the matrix cracks throughout the RVE, causing the ultimate fracture of the RVE. As for the case of transverse compression, matrix plastic damage first happens at the location where two fibers are closely adjacent in the direction perpendicular to the load. Then, more matrix cracks occur at different locations adjoining the fibers. And finally the matrix cracks at different locations are linked to form a main crack, having a certain angle with the loading direction. It can be concluded that the tension fracture is controlled by interfacial debonding and the compression failure is dominated by matrix plastic damage.

Acknowledgments

This work was supported by the National Natural Science Foundation of China (No. 11402045), the China Postdoctoral Science Foundation Funded Project (No. 2014M560204) and the Fundamental Research Funds for the Central Universities (No. DUT16LK35).

References

[1] C. Soutis. Fibre reinforced composites in aircraft construction. *Progress in Aerospace Sciences*, 41(2): 143-151, 2005.

[2] L.C. Hollaway. A review of the present and future utilisation of FRP composites in the civil infrastructu re with reference to their important in-service properties. *Construction and Building Materials*, 24(12): 2419-2445, 2010.

[3] C.A. Squires, K.H. Netting, and A.R. Chambers. Understanding the factors affecting the compressive testing of unidirectional carbon fibre composites. *Composites Part B*, 38: 481-487, 2007.

[4] X. Liu, R.G. Wang, Z.J. Wu, and W.B. Liu. The effect of triangle-shape carbon fiber on the flexural properties of the carbon fiber reinforced plastics. *Materials Letters*, 73: 21-23, 2012.

Excerpt from ISBN 978-3-00-053387-7

[5] R.G. Wang, X. Liu, and W.B. Liu. The B-basis value of the shearing strength of triangle-shape carbon fibers reinforced plastics. *Polymers and Polymer Composites*,19(4-5): 327-332, 2011.

[6] S.J. Park, M.K. Seo, and H.B. Shim. Effect of fiber shapes on physical characteristics of noncircular carbon fibers-reinforced composites. *Materials Science and Engineering: A*,352(1-2): 34-39, 2003.

[7] T.J. Kim and C.K. Park. Flexural and tensile strength developments of various shape carbon fiber-reinforced lightweight cementitious composites. *Cement and Concrete Research*, 28(7): 955-960, 1998.

[8] S.J. Park, M.K. Seo, H.B. Shim, and K.Y. Rhee. Effect of different cross-section types on mechanical properties of carbon fibers- reinforced cement composites. *Materials Science and Engineering: A*, 366(2): 348-355, 2004.

[9] Z.W. Xu, Y.D. Huang, L. Liu, et al. Surface characteristics of kidney and circular section carbon fibers and mechanical behavior of composites. *Materials Chemistry and Physics*, 106(1): 16-21, 2007.

[10] Z.W. Xu, J.L. Li, X.Q. Wu, et al. Effect of kidney-type and circular cross sections on carbon fiber surface and composite interface. *Composites Part A*, 39: 301-307, 2008.

[11] H.R. Pakravan, M. Jamshidi, M. Latif, and F. Pacheco-Torgal. Influence of acrylic fibers geometry on the mechanical performance of fiber-cement composites. *Journal of Applied Polymer Science*, 125(4): 3050-3057, 2012.

[12] M.M. Aghdam and A. Dezhsetan. Micromechanics based analysis of randomly distributed fiber reinforced composites using simplified unit cell model. *Composite Structures*, 71(3-4) 327-332, 2005.

[13] E.J. Barbero, G.F. Abdelal, and A. Caceres. A micromechanics approach for damage modeling of polymer matrix composites, *Composite Structures*, 67(4): 427-436, 2005.

[14] J. Segurado and J. LLorca. A computational micromechanics study of the effect of interface decohesion on the mechanical behavior of composites. *Acta Materialia*, 53(18): 4931-4942, 2005.

[15] T.J. Vaughan and C.T. McCarthy. Micromechanical modelling of the transverse damage behaviour in fibre reinforced composites. *Composite Science and Technology*, 71(3): 388-396, 2011.

[16] L. Yang, Y. Yan, Y.J. Liu, and Z.G. Ran. Microscopic failure mechanisms of fibre-reinforced polymer composites under transverse tension and compression. *Composite Science and Technology*, 72(15): 1818-1825, 2012.

[17] L. Yang, Y. Yan, Z.G. Ran, and Y.J. Liu. A new method for generating random fibre distributions for fibre reinforced composites. *Composite Science and Technology*, 76(4): 14-20, 2013.

[18] C. González and J. LLorca. Mechanical behavior of unidirectional fiber-reinforced polymers under transverse compression: Microscopic mechanisms and modeling. *Composite Science and Technology*, 67(13): 2795-2806, 2007.

Excerpt from ISBN 978-3-00-053387-7